RESEARCH ARTICLE

Chemical composition of indoor and outdoor PM$_{2.5}$ in the eastern Arabian Peninsula

Ersin Tutsak[1] · Balint Alfoldy[2] · Mohamed M. Mahfouz[1] · Jassem A. Al-Thani[1] · Oguz Yigiterhan[1] · Imran Shahid[1] · Rima J. Isaifan[3] · Mustafa Koçak[4]

Abstract

Water-soluble and trace metal species in fine particulate matter (PM$_{2.5}$) were determined for indoor and outdoor environments in Doha, Qatar. During the study period, PM$_{2.5}$ concentrations showed significant variability across several indoor locations ranging from 7.1 to 75.8 μg m^{-3}, while the outdoor mass concentration range was 34.7–154.4 μg m^{-3}. The indoor and outdoor PM$_{2.5}$ levels did not exhibit statistically significant correlation, suggesting efficient building envelope protection against outdoor PM$_{2.5}$ pollution. Rather than outdoor sources, human activities such as cooking, cleaning, and smoking were the most significant influence on chemical composition of indoor PM$_{2.5}$. NH$_4^+$ concentration was insufficient to neutralize SO$_4^{2-}$ indoors and outdoors, indicating the predominant presence of NH$_4$HSO$_4$. The enrichment factors indicated that outdoor Fe, Mn, Co, Cr, and Ni in PM$_{2.5}$ mostly originated from crustal sources. In contrast, the remaining outdoor trace metals (Cu, Zn, As, Cd, Pb, and V) were mainly derived from anthropogenic sources. The indoor/outdoor concentration ratios revealed significant indoor sources for NH$_4^+$ and Cu. The crustal matter, water-soluble ions, and sea salt explained 42%, 21%, and 1% of the indoor PM$_{2.5}$ mass, respectively. The same groups sequentially constituted 41%, 16%, and 1% of the outdoor PM$_{2.5}$ mass.

Keywords PM$_{2.5}$ · Indoor/outdoor · Chemical composition · Arabian Peninsula

Introduction

Particulate matter, particularly with a diameter less than 2.5 μm (PM$_{2.5}$), has adverse health effects, which can harm human cardiovascular and respiratory systems as well as the immune function (Lippmann 2014; Glencross et al. 2020; Yin et al. 2020). According to the World Health Organization (WHO), ambient air pollution was responsible for an estimated 4.2 million premature deaths worldwide in 2019. Therefore, accurately assessing air pollution levels is crucial

to evaluating health effects and associated costs. The impact of particulate matter on public health depends on its concentrations, chemical composition, particle size distribution, and superficial area (Valavanidis et al. 2008; Okuda 2013). Nonetheless, the chemical composition mainly determines the toxicity level of particulate matter (Park et al. 2018). Therefore, particulate matter mass concentrations and chemical composition should be evaluated together to explain their impacts on human health.

The Arabian Peninsula's air quality status is affected by various natural and anthropogenic emissions and meteorological conditions that generate complex temporal and spatial gradients. In addition to local pollution, the region is also affected by pollution transported from distant sources. Lelieveld et al. (2009) demonstrated the influence of long-range transport of air pollution from Europe and the Middle East and natural emissions in the region. Desert dust is the primary natural source of particulate matter over the Arabian Peninsula. However, Osipov et al. (2022) carried out shipborne measurements in the Arabian Peninsula. Their modeling results exhibited that hazardous fine particulate matter

---

✉ Ersin Tutsak
ersin@qu.edu.qa

[1] Environmental Science Center, Qatar University, Doha, Qatar

[2] Aerosol d.o.o., 1000 Ljubljana, Slovenia

[3] College of Science and Engineering, Hamad Bin Khalifa University, Doha, Qatar

[4] Nicosia, Cyprus

is mainly of anthropogenic origin (> 90%) and is distinctly different from that of less hazardous coarse desert dust particles. They showed that desert dust dominates both the fine and coarse aerosol size fractions, masking the human signal since most (53%) of the aerosol optical depth was caused by human-made particles. Accordingly, anthropogenic air pollution is a primary health concern in the Arabian Peninsula (Isaifan 2023). On the other hand, indoor particulate matter levels and their chemical composition are essential knowledge in regions such as Qatar, where people spend most of their time indoors, especially during hot days. People's welfare is tied to the quality of their living conditions, and as living standards rise, so do people's expectations for a healthy living environment. Considering these facts, this study aims to explore the chemical compositions of $PM_{2.5}$ indoor and outdoor mass concentration and their correlation in order to assist environmental regulators and policymakers in formulating recommendations and guidelines to safeguard the population from the adverse health effects of air pollution in Qatar.

Materials and methods

Sampling site and aerosol sampling

Qatar is a peninsula situated on the northeast coast of the Arabian Peninsula, bordered by Saudi Arabia from the south and surrounded by the Arabian Gulf on the east, north, and west. The country's surface area is 11,586 km^2 and its population stands at ~ 3 million as reported in 2023. The population has increased 1.5 times over the past 10 years. Doha, the capital city of Qatar, is bordered by industrialized areas 30 km to the north (Mesaieed) and 60 km to the south (Ras Laffan), where most of Qatar's oil and gas industry is situated. Furthermore, 12 km to the southwest, an industrial area with big smelting workshops is located. Apart from local emission sources, the city of Doha is also affected by air masses reaching from the Arabian Peninsula and the Arabian Gulf. These air masses may carry various natural and anthropogenic aerosols associated with mineral dust intrusions, petroleum industry, shipping activities, and sea spray (Javed et al. 2019; Javed and Guo 2020).

Indoor and outdoor $PM_{2.5}$ samples were simultaneously obtained from urban/arid Doha (Qatar) during two sampling campaigns that cover winter (from December to March) and transition (October–November and April–May) seasons. The first campaign commenced on 12 February and finished on 27 May 2018, while the second was carried out from 27 September to 3 November 2018. Correspondingly, a total of 36 and 18 $PM_{2.5}$ samples were collected for winter and transition periods. The sampling period for each sample varied from 2 to 7 days. From February 12 to 14 and October 14 to 18, no outdoor samples were collected due to a mechanical failure of the instrument. Except for Friday and Saturday, residential indoor and outdoor aerosol samples were continuously obtained. In contrast, indoor samplers from classes were exclusively operated for about 8 h a day during the classes throughout the five working days of the week. $PM_{2.5}$ sampling strategy designed (see Table 1) to reflect indoor air quality, including five homes (one of them being a smoker's home), four classrooms, a kindergarten reception area, laboratory, Qanat Quartier (seaside), and their corresponding outdoor samples (Fig. 1). Throughout the study period, indoor environment windows were kept closed.

Indoor and outdoor $PM_{2.5}$ aerosol sampling was simultaneously carried out by a volume Harvard impactor with a size-selective inlet. The instrument was operated at 10 L per minute in order to ensure a cutoff diameter of 2.5 μm with an efficiency of 50%. The atmospheric particles were collected on Teflon filters (Pall, Teflon Membrane Disc Filters, 37 mm diameter and 2-μm pore size). The filters were conditioned in desiccator chambers under controlled temperature and relative humidity ($T = 20\ °C$ and $RH = 40\%$) before and after the sampling. The mass of the filters was determined gravimetrically by a Mettler Toledo microbalance with a 0.1 μg readability. Before weighing, the static electrical charge of filters was neutralized by applying a Milty Zerostat 3 antistatic gun. The weight difference between the loaded and empty filters (net mass) was divided by the sampled air volume to calculate $PM_{2.5}$ masses for indoor and outdoor samples.

Analysis of elements and water-soluble ions

Half of the filters were extracted using 5 mL of HNO_3 (65% nitric acid) and 2 mL of HF (40% hydrofluoric acid). A total digestion procedure followed by inductively coupled plasma mass spectrometry (ICP-MS) was performed to measure elemental concentrations of Cr, Mn, Fe, Co, Ni, Cu, Zn, Al, V,

Table 1 Categorization of indoor and outdoor samples obtained from urban/arid Doha during 12 February–27 May 2018 and 27 September–3 November 2018

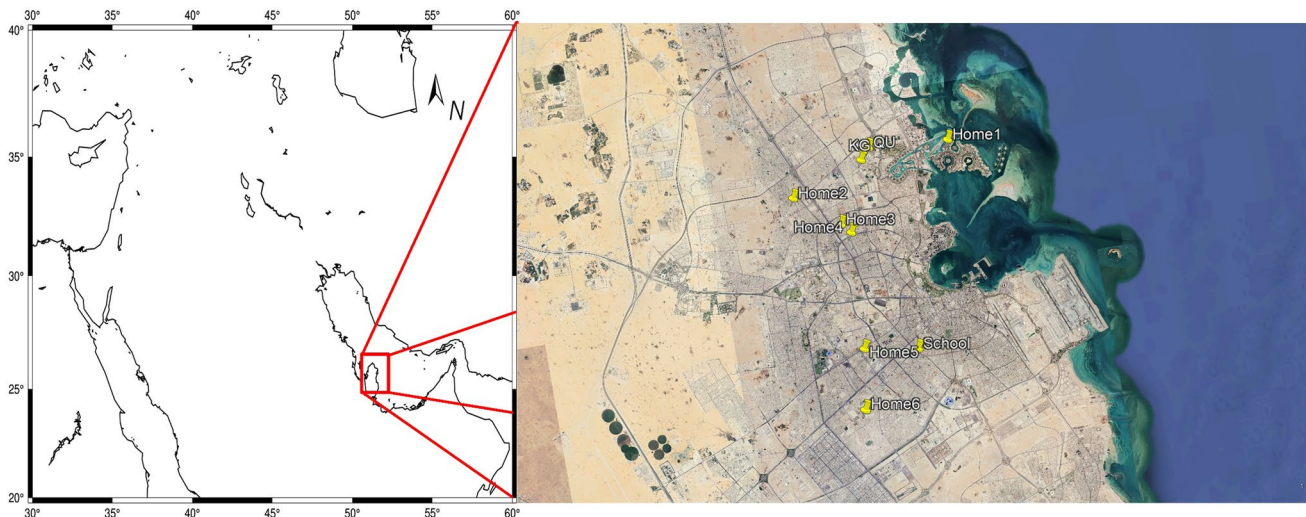| Site	Indoor	Indoor	Outdoor
Kindergarten	Class 1	Reception	Garden
School	Class 2	Class 3	Garden
Qanat Quartier seaside	Home 1	-	Balcony
Home-smoker	Home 2	-	Garden
Home-nonsmoker	Home 3	-	Garden
Home-nonsmoker	Home 4	-	Garden
Home-nonsmoker	Home 5	-	Garden
Home-nonsmoker	Home 6	-	Garden
Home-nonsmoker	Home 7	-	Garden
Qatar University	Class 4	Laboratory	Garden

Fig. 1 Location of sites where $PM_{2.5}$ samples were collected

As, Cd, and Pb in the aerosol samples, following the method described in detail by Yilmaz (2016). The detection limits (LOD), calculated as three times the standard deviation (3σ) of blanks, were 0.01 ng/m³ for Cd, V, As, and Co; 0.2 ng/m³ for Pb, Ni, Cu, Mn, and Cr; 10 ng/m³ for Zn and Fe; and 10 ng/m³ for Al. Analytical recoveries were better than 85% for Fe, Co, Ni, Cu, Cr, and As and higher than 90% for Al, Mn, Zn, Cd, Pb, and V. Blank contributions were found to be less than 8%.

In order to measure water-soluble ions (Cl^-, NO_3^-, SO_4^{2-}, Na^+, NH_4^+, K^+, Mg^{2+}, and Ca^{2+}), half of the filters were transferred into 20 mL vials, and 10 mL ultrapure Milli Q water (18.2 Ωm) was added in a laminar flow hood to avoid possible contamination. Samples were extracted for 60 min using a mechanic shaker, and after removing filters, 100 μL of chloroform was added to each bottle to prevent any biological activity. Before analysis, aliquots of samples were filtered by a nylon membrane syringe filter (0.45 μm; 25 mm diameter; VWR International). Water-soluble ions in $PM_{2.5}$ samples were analyzed by ion chromatography instrument (ICS-5000). Water-soluble cations (Na^+, NH_4^+, K^+, Mg^{2+}, and Ca^{2+}) were determined by using CS12A separation column, 20 mM MSA eluent, DRSC600 suppressor, and conductivity detector. Meanwhile, water-soluble anions (Cl^-, NO_3^-, SO_4^{2-}) were measured by using an AS-11 separation column, 12 mM NaOH eluent, DRSA600 suppressor, and conductivity detector as per the method reported in (Bardouki et al. 2003; Nehir and Koçak 2018). The detection limits for water-soluble ions were better than 1 ppb, and the blank contributions for all water-soluble ions were found to be less than 9%. Concentrations were corrected accordingly. The non-sea-salt fraction of water-soluble ions was determined using the following equation:

nss-Ion $= (Ion)_{aerosol} - (Ion/Na^+)_{seawater} \times (Na^+)_{aerosol}$. In this study, mass ratios of 0.119, 0.037, and 0.251 were used for $(Mg^{2+}/Na^+)_{seawater}$, $(K^+/Na^+)_{seawater}$, and $(SO_4^{2-}/Na^+)_{seawater}$, respectively (Millero 2006).

Calculation of the enrichment factor for trace elements

The enrichment factor (EF) was employed for distinguishing between natural and anthropogenic sources of trace metals. The EF is typically defined by the following equation:

$$EF = ([E]/[R])_{sample}/([E]/[R])_{crust}$$

where E represents the element of interest and R is the reference element for crustal material. $([E]/[R])_{sample}$ is the concentration ratio of E to R in the aerosol sample, and $([E]/[R])_{crust}$ is the average concentration ratio of E to R in the Earth's crust. In this study, Al was chosen as the reference element. The crustal ratios of the elements were obtained from Rudnick and Gao (2014). A trace metal in particulate matter is usually considered to have a significant crustal source if its crustal enrichment factor (EF) value is less than 10; on the other hand, a substantial portion of an element is thought to have a non-crustal source if its EF value is greater than 10 (Chester et al. 1999).

Statistical analysis

Data were statistically analyzed using SPSS 28 software, which included performing Pearson correlation analysis and principal component analysis with varimax rotation.

Table 2 Statistical summary of indoor and outdoor $PM_{2.5}$ ($\mu g\ m^{-3}$)

$PM_{2.5}$	Indoor	Outdoor	I/O
All	23.9 ± 16.3	76.9 ± 29.0	0.31
Classroom	14.4 ± 5.9		0.18
Reception	41.1 ± 33.5		0.53
Home	25.1 ± 5.8		0.32
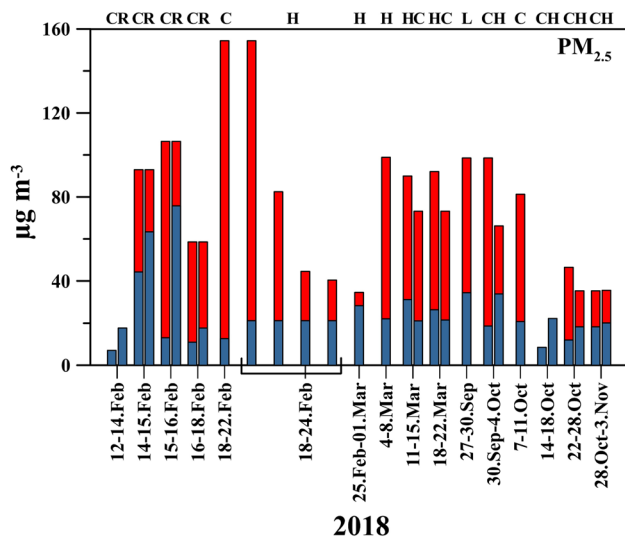
Fig. 2 Temporal variability of indoor (blue bar) and outdoor (red bar) $PM_{2.5}$. Explanation of abbreviation: Class (C), Home (H), Lab (L), and Reception (R)

Results and discussions

$PM_{2.5}$ mass

Table 2 shows the arithmetic mean concentrations of $PM_{2.5}$ along with the standard deviation for indoor and outdoor environments. Throughout the sampling campaign, indoor mass concentrations varied between 7.1 and 75.8 $\mu g\ m^{-3}$ (Fig. 2) with a mean value of $23.9 \pm 16.3\ \mu g\ m^{-3}$. Indoor $PM_{2.5}$ concentrations were found to be decreasing in the order Reception > Home > Classroom; $41.1 \pm 33.5\ \mu g\ m^{-3}$, $25.1 \pm 5.8\ \mu g\ m^{-3}$, and $14.4 \pm 5.9\ \mu g\ m^{-3}$, respectively, as can be shown in Table 2. In comparison, the outdoor $PM_{2.5}$ concentrations exhibited large variability ranging from 34.7 to 154.4 $\mu g\ m^{-3}$ (Fig. 2) with an arithmetic mean of $76.9 \pm 29.0\ \mu g\ m^{-3}$. The degree of relationship between indoor and outdoor pollutant levels has been attributed to infiltration rates, decay rates, and emissions from indoor sources (Meier et al. 2015). Except for the Reception site, the indoor and outdoor $PM_{2.5}$ levels did not show statistically significant correlation coefficients, suggesting efficient building envelope protection against

outdoor $PM_{2.5}$ pollution. The lowest I/O (0.08) ratio was observed during a dust event, and the highest ratio was monitored for smoker inhabitants with a value of 0.82, denoting the influence of smoking on indoor air quality. Correspondingly, the highest and lowest I/O were observed for Reception (0.53) and Classrooms (0.18) sites, followed by the Home (0.32) sites. Frequent door openings caused more exchange between the Reception site and the outdoor environment, resulting in higher $PM_{2.5}$ levels in the Reception site.

On all sampling days, the outdoor concentrations of $PM_{2.5}$ exceeded the WHO recommended limit for $PM_{2.5}$ (15 $\mu g\ m^{-3}$ for 24-h mean as per the 2021 standards). Saraga et al. 2017 reported the overall mean concentrations of 15.5 $\mu g/m^3$ and 172 $\mu g/m^3$ for indoor and outdoor $PM_{2.5}$, respectively, for the study period from April to June 2015 in Qatar. The present outdoor $PM_{2.5}$ average mean concentration was 2.2 times less than Saraga et al. (2017) reported. This discrepancy might be attributed to the dust events frequently occurring over the region during the spring and summer seasons (Farahat 2016). If the Reception site is not considered, this reported average indoor $PM_{2.5}$ in this study would generally agree with the indoor values reported in Saraga et al. (2017).

Water-soluble ions

Table 3 shows a statistical summary of the water-soluble ions attained from this study, including arithmetic mean concentrations and their standard deviations and minimum and maximum values. The indoor water-soluble ions were in the order $SO_4^{2-} > NH_4^+ > Ca^{2+} > NO_3^- > Cl^- > Na^+ > Mg^{2+} > K^+$, while the outdoor ions followed the decreasing order $SO_4^{2-} > Ca^{2+} > NH_4^+ > NO_3^- > Cl^- > Na^+ > Mg^{2+} > K^+$. The highest average indoor and outdoor concentrations were found for SO_4^{2-}, with values of 2.92 $\mu g\ m^{-3}$ and 7.87 $\mu g\ m^{-3}$, respectively.

It was followed by NH_4^+ indoors with a mean value of $0.72 \pm 0.47\ \mu g\ m^{-3}$, while Ca^{2+} was found to be the second highest outdoors with a mean of $2.23 \pm 1.06\ \mu g\ m^{-3}$. The most significant ions were SO_4^{2-} (62% indoor; 63% outdoor), NH_4^+ (15% indoor; 10% outdoor), Ca^{2+} (14% indoor; 17% outdoor), and NO_3^- (4% indoor; 5% outdoor) contributing 95% to the total ion mass. The contributions of Cl^-, Na^+, Mg^{2+}, and K^+ to indoor and outdoor ion mass were small of only 2%, 1%, 1%, and 1%, respectively. The water-soluble ion concentrations in our $PM_{2.5}$ samples were lower than those previously reported in Qatar (Saraga et al. 2017; Javed and Guo 2020). For instance, the values of 4.82 $\mu g\ m^{-3}$ and 15.24 $\mu g\ m^{-3}$ were reported by Saraga et al. (2017) for indoor and outdoor SO_4^{2-}, respectively. This difference may be attributed to the length of the sampling campaigns.

The temporal variations of indoor and outdoor water-soluble ion concentrations throughout the sampling periods

Table 3 Statistical summary for the water-soluble ions in $PM_{2.5}$ ($\mu g\ m^{-3}$)

Variable	Indoor			Outdoor		
	Mean ± std	Minimum	Maximum	Mean ± std	Minimum	Maximum
Na^+	0.05 ± 0.04	0.01	0.16	0.18 ± 0.10	0.06	0.40
NH_4^+	0.72 ± 0.47	0.20	2.07	1.17 ± 0.88	0.25	2.80
K^+	0.02 ± 0.01	0.00	0.04	0.06 ± 0.03	0.02	0.15
Mg^{2+}	0.03 ± 0.02	0.00	0.12	0.11 ± 0.05	0.05	0.23
Ca^{2+}	0.69 ± 0.95	0.08	4.40	2.23 ± 1.06	0.64	4.38
Cl^-	0.12 ± 0.10	0.03	0.39	0.24 ± 0.22	0.04	0.73
NO_3^-	0.18 ± 0.12	0.04	0.51	0.69 ± 0.55	0.08	1.85
SO_4^{2-}	2.92 ± 1.95	0.51	7.86	7.87 ± 4.82	2.55	19.67
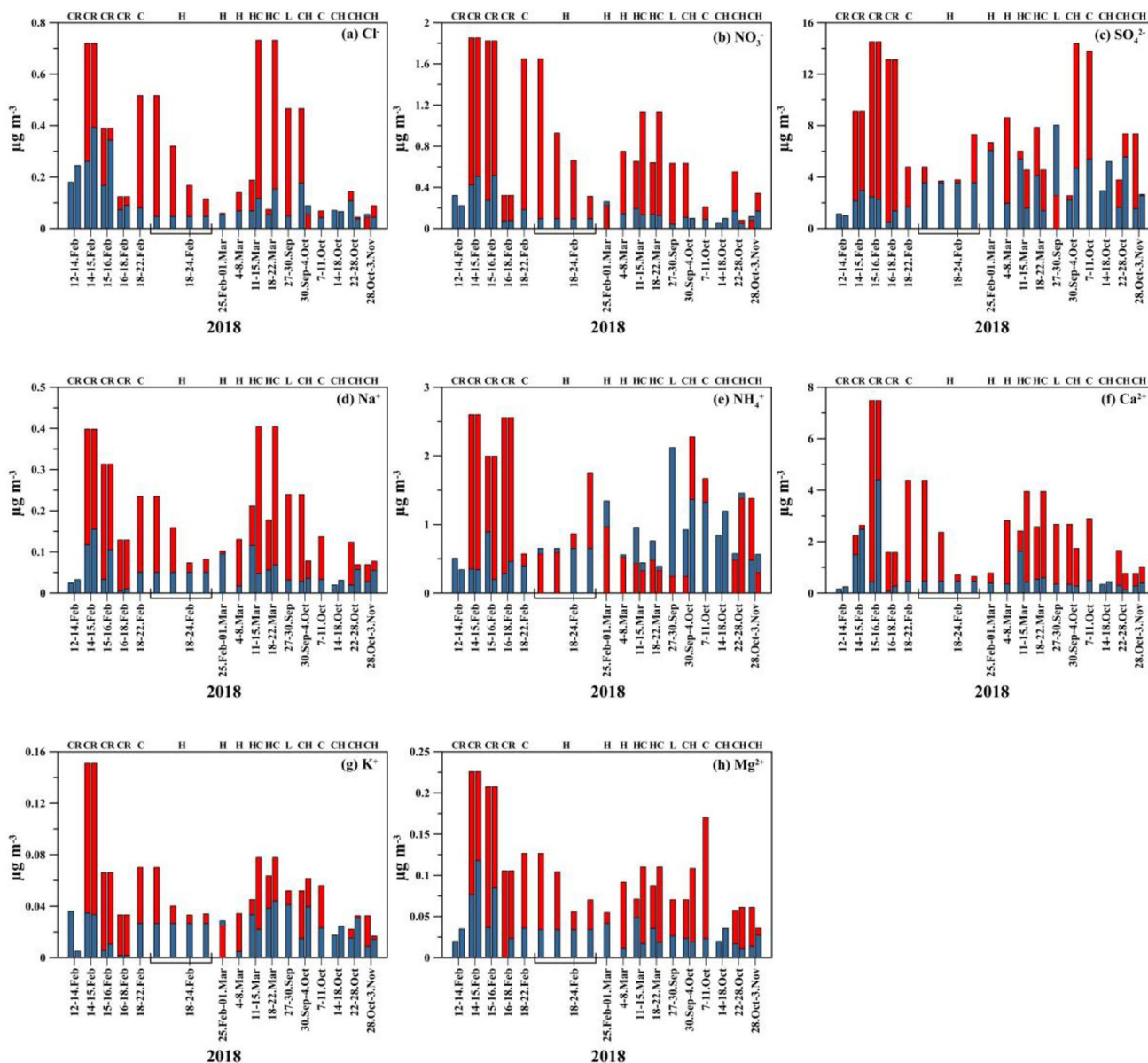
Fig. 3 Temporal variability of indoor (blue bar) and outdoor (red bar): **a** Cl^-, **b** NO_3^-, **c** SO_4^{2-}, **d** Na^+, **e** NH_4^+, **f** Ca^{2+}, **g** K^+, and **h** Mg^{2+} in $PM_{2.5}$. Explanation of abbreviation: Class (C), Home (H), Lab (L), and Reception (R)

are depicted in Fig. 3. The results revealed significant fluctuations in the daily concentrations of water-soluble ions. This type of variability suggested the influence of various sources of the observed levels. Table 1S presents the indoor and outdoor correlations between water-soluble ions. As anticipated, sea salt species (Na^+, Cl^- and Mg^{2+}) showed high correlation in both indoor and outdoor, indicating they were mainly originated from sea salt. NH_4^+ was strongly correlated with SO_4^{2-} ($r = 0.91$ for indoor, $r = 0.83$ for outdoor), demonstrating the formation of ammonium sulfate. Nevertheless, the analyzed regression revealed that NH_4^+ is insufficient to neutralize SO_4^{2-}. This might be related to the main presence of NH_4HSO_4 instead of $(NH_4)_2SO_4$ (Koçak et al. 2004). The correlation between Ca^{2+} and NO_3^- was significant indoors and outdoors, indicative of the existence of $Ca(NO_3)_2$. Figure 4a, b shows the biplot of PCA for indoor and outdoor trace metals. PCA results showed that the first two components accounted for about 83.3% (indoor) and 84.7% (outdoor) of the total variance. PC1 and PC2 explained 52.6% (indoor) and 30.7% (indoor) and 50.7% (outdoor) and 34.0% (outdoor) of the total variance, respectively. Specifically, Cl^-, NO_3^-, Na^+, Mg^{2+}, and Ca^{2+} played significant roles in PC1, with loading coefficients greater than 0.65. The effects of SO_4^{2-} and NH_4^+ were significant in P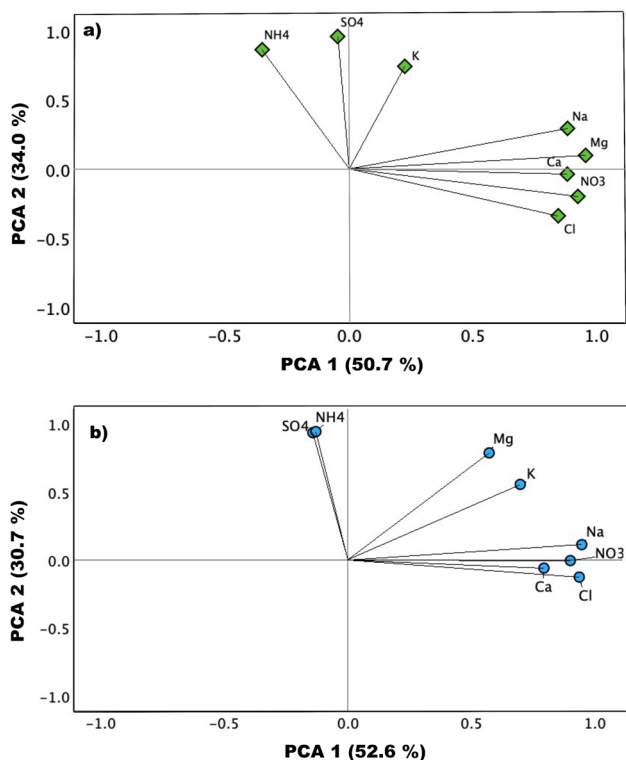C2, with loading coefficients exceeding 0.90. The main sources of the ions in PC1 for both indoor and outdoor were natural sources (crustal and sea salt), whereas those in PC2 were related to gas to particle secondary aerosols sources.

Trace metal species

Figure 5 shows the indoor and outdoor temporal fluctuations in the concentrations of metals in $PM_{2.5}$ throughout the study period. Table 4 presents a static summary of trace metal species. The dominant trace metals in $PM_{2.5}$ were Al (612 ± 416 ng m^{-3}), Fe (314 ± 243 ng m^{-3}), and Zn (27.8 ± 13.4 ng m^{-3}) indoors, whereas Al (2696 ± 1907 ng m^{-3}), Fe (1545 ± 1064 ng m^{-3}), and Zn (49.5 ± 37.9 ng m^{-3}) were predominant in outdoors. It is apparent from the results that crustal metal species, namely, Al and Fe, exhibited higher concentrations, comprising 93% and 97% of the measured indoor and outdoor trace metal masses, respectively. In the indoor environment, the trace metals exhibited the following descending order: Al > Fe > Zn > Cu > Ni > Mn > V > Cr > Pb > As > Co > Cd. Correspondingly, the outdoor trace metals followed the decreasing order of Al > Fe > Zn > Mn > V > Ni > Cr > Pb > Cu > As > Co > Cd. The levels of outdoor trace metal concentrations were consistent with the findings of the previous study in Qatar (Javed and Guo 2020). Furthermore, they reported similar arithmetic mean concentrations for Co, Cd, and Pb. In contrast, the mean concentrations of crustal species such as Al, Fe, and Mn were inconsistent with those observed in our study. This disparity could mainly be attributed to variations in the strength of dust emissions during the respective sampling periods.

The correlation coefficients for trace metal species are presented in Table S2a and S2b for indoor and outdoor particles, respectively. As expected, there was a strong correlation between the crustal species (Al, Mn, and Fe) outdoors. Additionally, Co and Cr were strongly correlated with crustal species outdoors, while Ni was moderately correlated. This implies that a substantial proportion of the measured outdoor concentrations of these Co, Cr, and Ni elements were associated with the crustal materials. On the other hand, the strength of the correlations between crustal species and all other trace metals, excluding Cu, increased significantly in the indoor environment compared to the outdoor environment. This may be attributed to the resuspension of the particles from the floor surfaces due to active human activities such as walking and vacuum cleaning (Abt et al. 2000; Wang et al. 2021). The lower increment in the indoor correlations of Cu with crustal species may imply a different indoor source for Cu (please see the "Relationship between indoor and outdoor for measured species" section).

Figure 6a, b shows the biplot of PCA for outdoor trace metals. PCA results indicated that the first three components accounted for approximately 91.5% of the total variance.
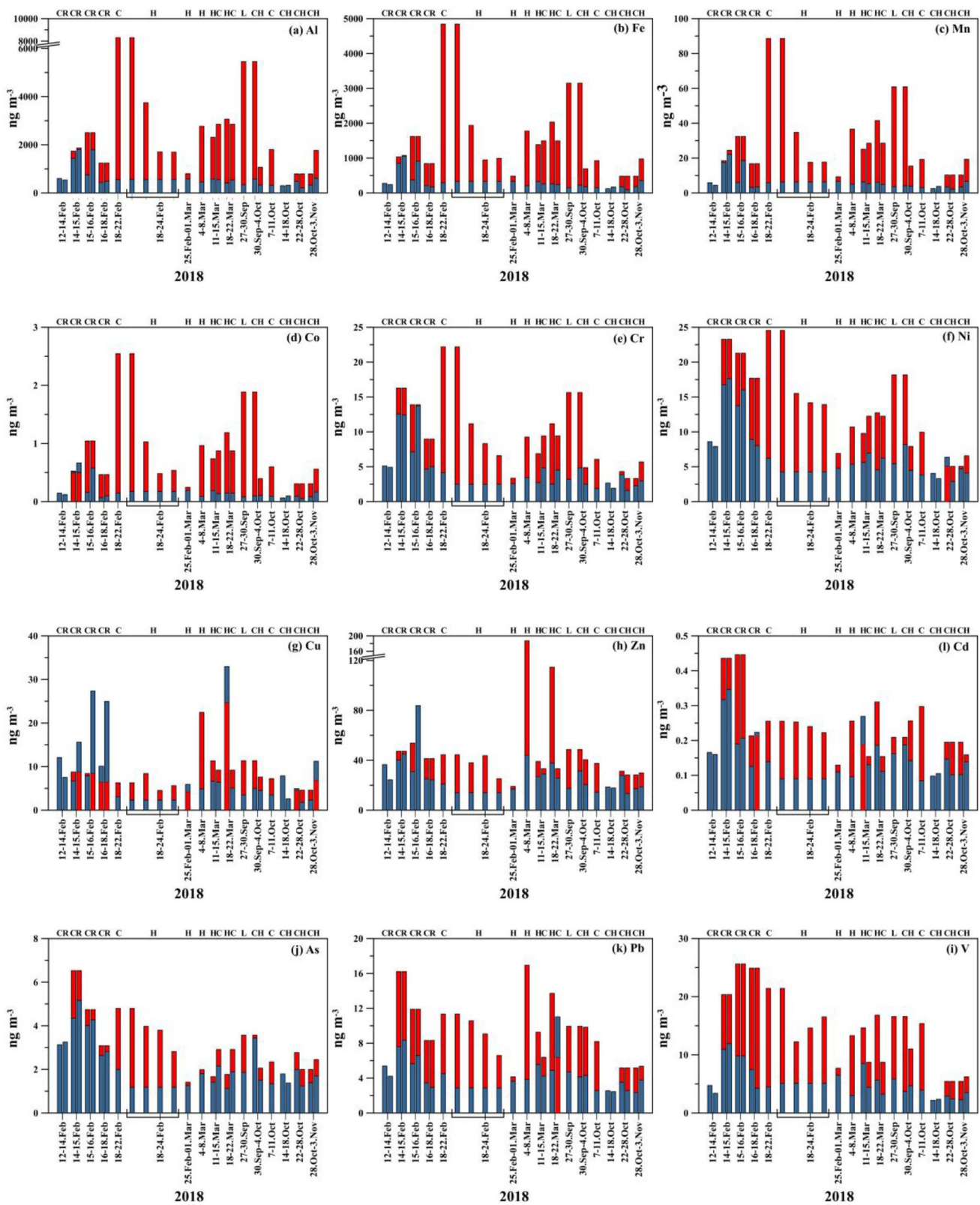

Fig. 4 Principal component analysis (PCA) biplots for **a** indoor and **b** outdoor ions in $PM_{2.5}$, based on the first two principal components, PCA1 and PCA2

Fig. 5 Temporal variability of indoor (blue bar) and outdoor (red bar) trace metals **a** Al, **b** Fe, **c** Mn, **d** Co, **e** Cr, **f** Ni, **g** Cu, **h** Zn, **i** Cd, **j** As, **k** Pb, and **l** V in $PM_{2.5}$. Explanation of abbreviation: Class (C), Home (H), Lab (L), and Reception (R)

Table 4 Statistical summary for the metal species in PM$_{2.5}$ (ng m^{-3})

Variable	Indoor			Outdoor		
	Mean ± std	Minimum	Maximum	Mean ± std	Minimum	Maximum
Al	612 ± 416	211	1804	2696 ± 1907	791	8310
Fe	314 ± 243	94	1055	1545 ± 1064	483	4843
Mn	6.3 ± 5.0	2.3	22.2	29.8 ± 19.8	9.3	88.6
Co	0.17 ± 0.16	0.05	0.67	0.86 ± 0.56	0.25	2.55
Cr	4.6 ± 3.3	1.6	13.7	9.5 ± 5.0	3.3	22.2
Ni	7.3 ± 4.2	2.9	17.6	13.6 ± 5.6	5.0	24.5
Cu	8.7 ± 8.0	1.8	33.0	9.0 ± 5.5	4.2	24.7
Zn	27.8 ± 14.6	13.4	83.9	49.5 ± 37.9	19.1	187.2
V	5.3 ± 2.8	2.2	11.9	15.2 ± 5.7	5.4	25.6
As	2.3 ± 1.1	1.1	5.2	3.0 ± 1.4	1.4	6.5
Pb	4.5 ± 2.0	2.4	11.0	9.1 ± 3.7	4.0	16.9
Cd	0.16 ± 0.07	0.16	0.35	0.23 ± 0.09	0.11	0.45

Fig. 6 Principal component analysis (PCA) biplots for outdoor metals in PM$_{2.5}$, based on **a** PCA 1 and PCA 2 and **b** PCA 1 and PCA 3
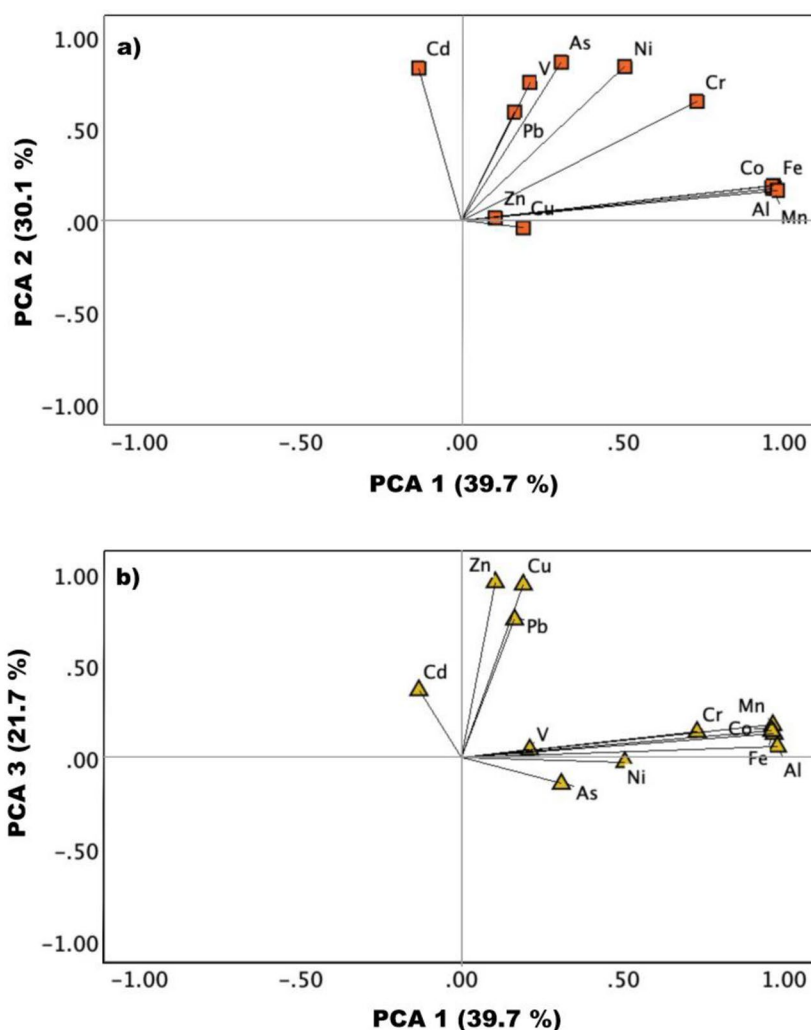
Specifically, PC1, PC2, and PC3 explained 39.7%, 30.1%, and 21.7% of the total variance, respectively. In PC1, Mn, Fe, Co, Al, and Cr had a significant effect, with loading coefficients greater than 0.73. These elements in aerosols mainly come from crustal sources. PC2 was related to Ni, V, As, and Cd, with loading coefficients above 0.90,

representing emissions from heavy oil combustion and industrial activities (Masiol et al. 2017; Squizzato et al. 2017). Ni and V are mainly derived from shipping emissions if the V/Ni ratio in PM$_{2.5}$ is greater than 0.7 (Zhang et al. 2014). The average outdoor V/Ni ratio from our study was 1.16 ± 0.29, indicating a significant contribution from shipping emissions. PC3 was associated with Cu, Zn, and Pb, with loading coefficients above 0.75. Cu, Zn, and Pb are indicators of traffic emissions, including brake, tire, and road wear, exhaust, and road dust (Tan et al. 2014; Crilley et al. 2017).

PCA results for indoor trace metals indicated that only one component could be extracted. Except for Cu, all metal species played a significant role in this component, with loading factors higher than 0.65, explaining 75% of the total variance.

Figure 7 shows EF for indoor and outdoor samples. Outdoor EF values for Fe, Mn, and Co were less than 2, while for Cr and Ni, they were approximately equal to 10, implying that these species found in PM$_{2.5}$ mainly originated from crustal sources. However, the outdoor EF values of 10 for Cr and Ni may also suggest significant enrichments compared to the EF values of Fe, Mn, and Co. Additionally, Fe, Mn, and Co indoor EF values remained under 2. In contrast, indoor EF for Cr and Ni exceeded 10, suggesting that anthropogenic sources contributed noteworthy to indoor Cr and Ni concentrations. For the remaining elements, namely, As, Pb, Cd, V, Zn, and Cu, EF values for indoor and outdoor samples were considerably above 10, indicating significant enrichments. It is worth noting that indoor enrichments for all species except Fe, Mn, and Co were higher than outdoor
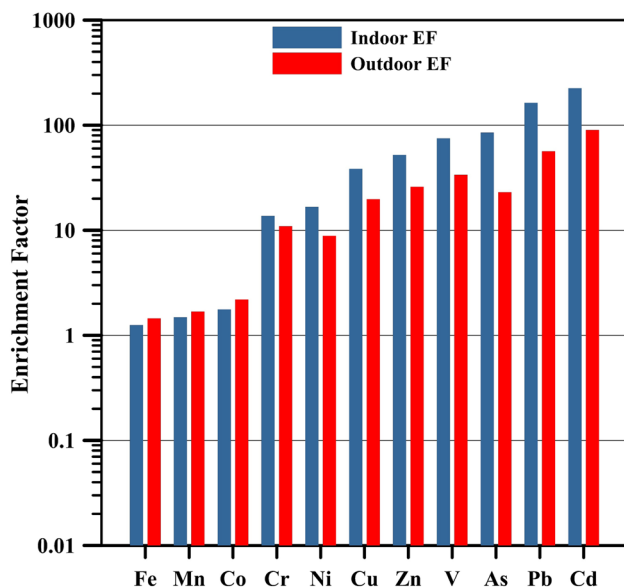
enrichments. Trace metals such as V, Cr, Mn, Fe, Ni, Cu, Pb, and Zn in particulate matter have the potential to be harmful, according to toxicological research (Rönkkö et al. 2018; Huang et al. 2022). WHO (2000) recommended the values of 5 ng m^{-3} and 150 ng m^{-3} for Cd and Mn, respectively, regardless of where these metals are found in PM$_{2.5}$ or PM$_{10}$ as thresholds to avoid harmful impacts. The results obtained from the present study for Cd and Mn were reasonably lower than the recommended values.

Relationship between indoor and outdoor for measured species

To evaluate spatial variations between indoor and outdoor environments, the coefficients of divergence (CD) for each pair of measured species were computed (Wongphatarakul et al. 1998). When the two sampling environments exhibit similarity, the CD values approach zero. On the other hand, CD values greater than 0.2 indicate spatial heterogeneity (Wilson et al. 2005; Krudysz et al. 2009). Figure 8 shows a lognormal plot of indoor-to-outdoor water-soluble (a) and (b) elemental metal concentrations with the averaged CD values. This study calculated the mean CD values of 0.42 and 0.28 for water-soluble ions and trace metals, respectively. These calculated CD values revealed a significant heterogeneous spatial distribution of water-soluble ions and trace metals between indoors and outdoors. All indoor species concentrations were found to be lower than those in outdoors (Fig. 8). It can be observed that there was a relatively high I/O ratio for NH$_4^+$ and Ca^{2+}, indicating the different sources of these two ions (Fig. 8a). The high indoor NH$_4^+$ levels may be related to ammonium salts formed indoors by the reaction between inorganic/organic acids and NH$_3$. It was reported that indoor NH$_3$ levels are frequently greater than outdoor ones (Ampollini et al. 2019; Li et al. 2020). Indoor ammonia may be emitted from cleaning agents, smoking, building materials, cooking, and the human body through breath, urine, and sweat (Nazaroff and Weschler 2020). For indoor Ca^{2+}, sources may be governed by the outdoor resuspension of crustal material from floor surfaces during household activities such as walking and vacuum cleaning or by its enhanced outdoor penetration on high windy days. Trace metals of crustal origin, such as Al, Fe, Mn, and Co, exhibited comparable average I/O ratios, implying common sources (Fig. 8b). In contrast, anthropogenic elements (Cr, As, Pb, Cd, V, Ni, Zn, and Cu) displayed variable I/O values, denoting distinct indoor sources. Notably, Cu demonstrated the highest I/O ratio, suggesting the presence of potential indoor sources. These indoor sources may include emissions generated by indoor electric universal motors found in appliances like vacuum cleaners, food processors, air dryers, and AC units (Szymczak et al. 2007; Hasheminassab et al. 2014; Vicente et al. 2020).
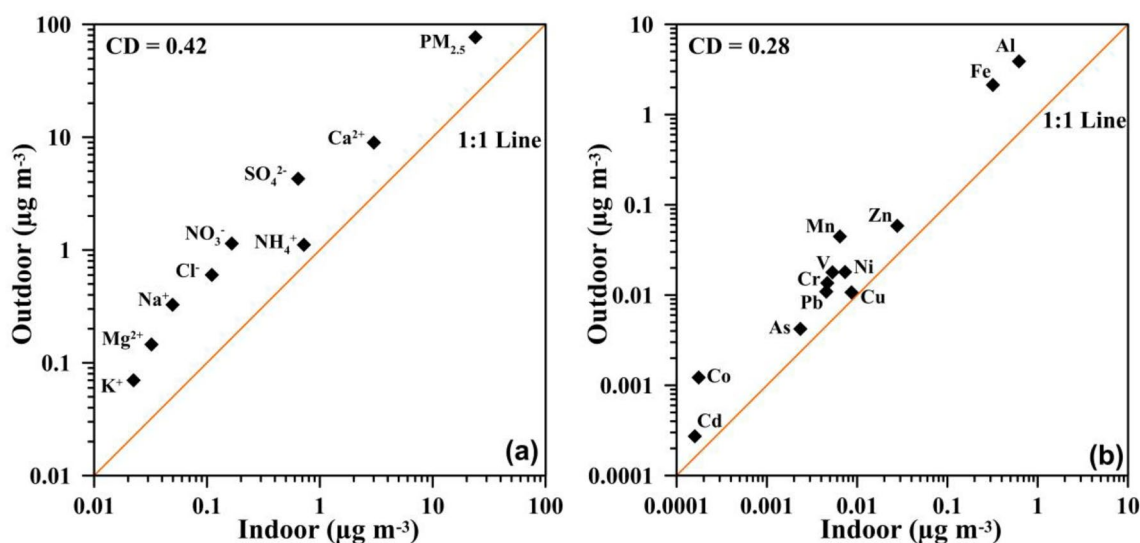

Fig. 7 Enrichment factor of trace metal species in indoor and outdoor PM$_{2.5}$ samples

Fig. 8 Comparison of average water-soluble ion and elemental metal concentrations between **a** indoor and **b** outdoor environments with the coefficients of divergence

Mass closure

Chemical mass closure calculations were performed for the indoor and outdoor PM$_{2.5}$. For that purpose, the chemical compositions of indoor and outdoor PM$_{2.5}$ mass were divided into four groups: crustal, sea salt, ions, and an undefined group. The total amount of crustal material was calculated by summing Al$_2$O$_3$, SiO$_2$, CO$_3^{2-}$, Fe, K, Mg, and Mn (Saraga et al. 2017). Al concentration was multiplied by the factor of 1.89 to obtain Al$_2$O$_3$, whereas SiO$_2$ was found by multiplying derived Al$_2$O$_3$ by 3. Ca was multiplied by 1.5 to account for CO$_3^{2-}$. The sea salt contribution was evaluated from Na$^+$ concentration, assuming that Na$^+$ originates merely from sea salt (Turekian 1976; Koçak et al. 2016). Ionic mass was the sum of nssSO$_4^{2-}$, NO$_3^-$, NH$_4^+$, nssK$^+$, and nssMg^{2+}. Figure 9 presents a mass closure analysis for indoor and outdoor PM$_{2.5}$. The figure

shows that the crustal material and water-soluble ions were identified as the primary contributors to total particulate mass, with percentages of 42% and 21% indoors and 41% and 16% outdoors, respectively. The ionic mass contribution for indoors increased by 5% compared to the outdoors. The largest ionic contributor to both indoor and outdoor PM$_{2.5}$ mass was SO$_4^{2-}$ (16% indoor; 13% outdoor), followed by NH$_4^+$ (4% indoor; 2% outdoor). The contribution of sea salt was found to be the smallest, accounting for 1% of the total mass for both indoor and outdoor. The undefined percentage for indoor mass concentration was 37%, while it was 43% for outdoor. These unidentified groups might be mainly attributed to the mass associated with black carbon and organic carbon, which was not measured in this study. The findings of the mass closure results did not align with the previous studies conducted in Qatar by Saraga et al. (2017) and Javed and Guo (2020),

Fig. 9 Mass closure analysis for indoor and outdoor PM$_{2.5}$
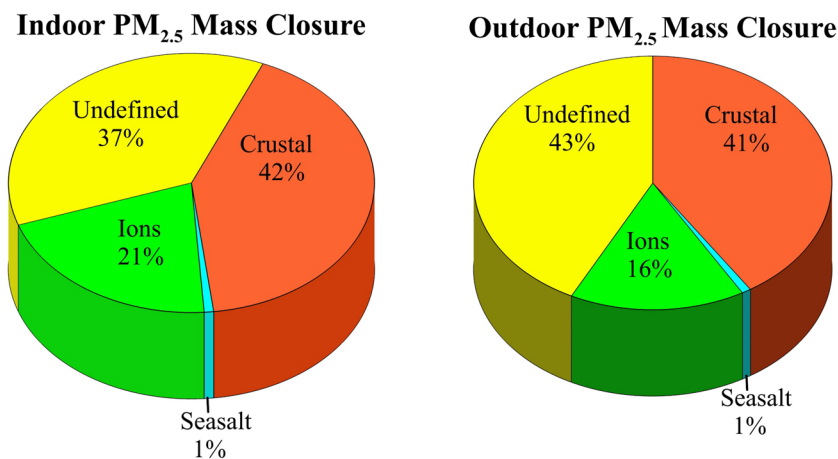
who reported 14% and 24% crustal material contributions to outdoor PM$_{2.5}$, respectively. In contrast, a more recent study conducted by Osipov et al. (2022) showed a 52% contribution of mineral dust to PM$_{2.5}$ mass in the region.

Summary and conclusion

This study revealed indoor and outdoor PM$_{2.5}$ concentrations and its chemical composition in Doha, Qatar, during the winter and transition seasons in 2018. Throughout the study period, there was a notable fluctuation in PM$_{2.5}$ concentrations within indoor locations, ranging from 7.1 to 75.8 µg m^{-3}. Outdoor mass concentrations also varied, varying from 34.7 to 154.4 µg m^{-3}. Indoor PM$_{2.5}$ levels were mainly governed by indoor sources instead of infiltration from outdoor sources. Concerning improving indoor air quality, air purification and ventilation systems are recommended as possible mitigation strategies. Extended sampling periods are necessary to understand the atmospheric particulate matter environment and climatology in the eastern Arabian Peninsula.

Declarations

Ethical approval Not applicable.

Consent to participate Not applicable.

Consent for publication Not applicable.

Competing interests The authors declare no competing interests.

References

Abt E, Suh HH, Catalano P, Koutrakis P (2000) Relative contribution of outdoor and indoor particle sources to indoor concentrations. Environ Sci Technol 34(17):3579–3587. https://doi.org/10.1021/es990348y

Ampollini L, Katz EF, Bourne S, Tian Y, Novoselac A, Goldstein AH, Lucic G, Waring MS, DeCarlo PF (2019) Observations and contributions of real-time indoor ammonia concentrations during HOMEChem. Environ Sci Technol 53:8591–8598. https://doi.org/10.1021/acs.est.9b02157

Bardouki H, Liakakou H, Economou C, Sciare J, Smolik J, Zdimal V, Eleftheriadis K, Lazaridis M, Dye C, Mihalopoulos N (2003) Chemical composition of size resolved atmospheric aerosols in the eastern Mediterranean during summer and winter. Atmos Environ 37:195–208. https://doi.org/10.1016/S1352-2310(02)00859-2

Chester R, Nimmo M, Preston MR (1999) The trace metal chemistry of atmospheric dry deposition samples collected at Cap Ferrat: a coastal site in the Western Mediterranean. Mar Chem 68:15–30. https://doi.org/10.1016/S0304-4203(99)00062-6

Crilley LR, Lucarelli F, Bloss WJ, Harrison RM, Beddows DC, Calzolai G, Nava S, Valli G, Bernardoni V, Vecchi R (2017) Source apportionment of fine and coarse particles at a roadside and urban background site in London during the 2012 summer ClearfLo campaign. Environ Pollut 220:766–778. https://doi.org/10.1016/j.envpol.2016.06.002

Farahat A (2016) Air pollution in the Arabian Peninsula (Saudi Arabia, the United Arab Emirates, Kuwait, Qatar, Bahrain, and Oman): causes, effects, and aerosol categorization. Arab J Geosci 9:196. https://doi.org/10.1007/s12517-015-2203-y

Glencross DA, Ho TR, Camiña N, Hawrylowicz CM, Pfeffer PE (2020) Air pollution and its effects on the immune system. Free Radic Biol Med 151:56–68. https://doi.org/10.1016/j.freeradbiomed.2020.01.179

Hasheminassab S, Daher N, Shafer MM, Schauer JJ, Delfino RJ, Sioutas C (2014) Chemical characterization and source apportionment of indoor and outdoor fine particulate matter (PM2.5) in retirement communities of the Los Angeles Basin. Sci Total Environ 490:528–537. https://doi.org/10.1016/j.scitotenv.2014.05.044

Huang C, Zhang L, Meng J, Yunjiang YY, Qi J, Shen P, Li X, Ding P, Chen M, Hu G (2022) Characteristics, source apportionment and health risk assessment of heavy metals in urban road dust of the Pearl River Delta, South China. Ecotoxicol Environ Saf 36:113490. https://doi.org/10.1016/j.ecoenv.2022.113490

Isaifan RJ (2023) Air pollution burden of disease over highly populated states in the Middle East. Front Public Health 10:1002707. https://doi.org/10.3389/fpubh.2022.1002707

Javed W, Guo B (2020) Chemical characterization and source apportionment of fine and coarse atmospheric particulate matter in

Doha, Qatar. Atmos Pollut Res 12(2):122–136. https://doi.org/10.1016/j.apr.2020.10.015

Javed W, Iakovides M, Garaga R, Stephanou EG, Kota SH, Ying Q, Wolfson JM, Koutrakis P, Guo B (2019) Source apportionment of organic pollutants in fine and coarse atmospheric particles in Doha, Qatar. J Air Waste Manage Assoc 69:1277–1292. https://doi.org/10.1080/10962247.2019.1640803

Koçak M, Kubilay N, Mihalopoulos N (2004) Ionic composition of lower tropospheric aerosols at a Northeastern Mediterranean site: implications regarding sources and long-range transport. Atmos Environ 38:2067–2077. https://doi.org/10.1016/j.atmosenv.2004.01.030

Koçak M, Mihalopoulos N, Tutsak E, Theodosi C, Zarmpas P, Kalegeri P (2016) PM10 and $PM_{2.5}$ composition over the Central Black Sea: origin and seasonal variability. Environ Sci Pollut Res 22(22):18076–18092. https://doi.org/10.1007/s11356-015-4928-2

Krudysz M, Moore K, Geller M, Sioutas C, Froines J (2009) Intra-community spatial variability of particulate matter size distributions in Southern California/Los Angeles. Atmos Chem Phys 9:1061–1110. https://doi.org/10.5194/acp-9-1061-2009

Lelieveld J, Hoor P, Jöckel P, Pozzer A, Hadjinicolaou P, Cammas JP, Beirle S (2009) Severe ozone air pollution in the Persian Gulf region. Atmos Chem Phys 9:1393–1406. https://doi.org/10.5194/acp-9-1393-2009

Li M, Weschler CJ, Bekö G, Wargocki P, Lucic G, Williams J (2020) Human ammonia emission rates under various ındoor environmental conditions. Environ Sci Technol 54(9):5419–5428. https://doi.org/10.1021/acs.est.0c00094

Lippmann M (2014) Toxicological and epidemiological studies of cardiovascular effects of ambient air fine particulate matter (PM2.5) and its chemical components: coherence and public health implications. Crit Rev Toxicol 44(4):299–347. https://doi.org/10.3109/10408444.2013.861796

Masiol M, Hopke PK, Felton HD, Frank BP, Rattigan OV, Wurth MJ, LaDuke GH (2017) Source apportionment of PM2.5 chemically speciated mass and particle number concentrations in New York City. Atmos Environ 148:215–229. https://doi.org/10.1016/j.atmosenv.2016.10.044

Meier R, Eeftens M, Phuleria HC, Ineichen A, Corradi E, Davey M, Fierz M, DucretStich RE, Aguilera I, Schindler C, Rochat T, Probst-Hensch N, Tsai MY, Kunzli N (2015) Differences in indoor versus outdoor concentrations of ultrafine particles, PM2.5, PM absorbance and NO_2 in Swiss homes. J Expo Sci Environ Epidemiol 25:499–505. https://doi.org/10.1038/jes.2015.3

Millero FJ (2006) Chemical oceanography. 3rd ed. CRC Press, pp 530 https://doi.org/10.1201/9780429258718

Nazaroff WW, Weschler CJ (2020) Indoor acids and bases. Indoor Air 30:559–644. https://doi.org/10.1111/ina.12670

Nehir M, Koçak M (2018) Atmospheric WSON in the Eastern Mediterranean. Atmos Chem Phys 18:3603–3618. https://doi.org/10.5194/acp-18-3603-2018

Okuda T (2013) Measurement of the specific surface area and particle size distribution of atmospheric aerosol reference materials. Atmos Environ 75:1–5. https://doi.org/10.1016/j.atmosenv.2013.04.033

Osipov S, Chowdhury S, Crowley JN et al (2022) Severe atmospheric pollution in the Middle East is attributable to anthropogenic sources. Commun Earth Environ 3(1):1–10. https://doi.org/10.1038/s43247-022-00514-6

Park M, Joo HS, Lee K et al (2018) Differential toxicities of fine particulate matter from various sources. Sci Rep 8:17007. https://doi.org/10.1038/s41598-018-35398-0

Rönkkö TJ, Jalava PI, Happo MS, Kasurinen S, Sippula O, Leskinen A, Hirvonen MR (2018) Emissions and atmospheric processes influence the chemical composition and toxicological properties of urban air particulate matter in Nanjing, China. Sci Total Environ 639:1290–1310. https://doi.org/10.1016/j.scitotenv.2018.05.260

Rudnick RL, Gao S (2014) Composition of the continental crust, in: Treatise on geochemistry. Elsevier, pp. 1–51. https://doi.org/10.1016/B978-0-08-095975-7.00301-6

Saraga D, Maggos T, Sadoun E, Fthenou E, Hassan H, Tsiouri V, Karavoltsos S, Sakellari A, Vasilakos C, Kakosimos K (2017) Chemical characterization of indoor and outdoor particulate matter (PM2.5, PM10) in Doha. Qatar Aerosol Air Qual Res 17:1156–1168. https://doi.org/10.4209/aaqr.2016.05.0198

Squizzato S, Cazzaro M, Innocente E, Visin F, Hopke PK, Rampazzo G (2017) Urban air quality in a mid-size city - PM2.5 composition, sources and identification of impact areas: from local to long range contributions. Atmos Res 186:51–62. https://doi.org/10.1016/j.atmosres.2016.11.011

Szymczak W, Menzel N, Keck L (2007) Emission of ultrafine copper particles by universal motors controlled by phase angle modulation. J Aerosol Sci 38:520–531. https://doi.org/10.1016/j.jaerosci.2007.03.002

Tan JH, Duan JC, Ma YL, Yang FM, Cheng Y, He KB, Yu YC, Wang JW (2014) Source of atmospheric heavy metals in winter in Foshan, China. Sci Total Environ 493:262–270. https://doi.org/10.1016/jscitotenv.2014.05.147

Turekian KK (1976) Oceans. Prentice-Hall, Englewood Cliffs

Valavanidis A, Fiotakis K, Vlachogianni T (2008) Airborne particulate matter and human health: toxicological assessment and importance of size and composition of particles for oxidative damage and carcinogenic mechanisms. J Environ Sci Heal Part C 26:339–362. https://doi.org/10.1080/10590500802494538

Vicente ED, Vicente AM, Evtyugina M, Calvo AI, Oduber F, Alegre CB, Castro A, Fraile R, Nunes T, Lucarelli F, Calzolai G, Nava S, Alves CA (2020) Impact of vacuum cleaning on indoor air quality. Build Environ 180:107059. https://doi.org/10.1016/j.buildenv.2020.107059

Wang B, Tang Z, Li Y, Cai N, Hu X (2021) Experiments and simulations of human walking-induced particulate matter resuspension in indoor environments. J Clean Prod 295:126488. https://doi.org/10.1016/j.jclepro.2021.126488

Wilson JG, Kingham S, Pearce J, Sturman AP (2005) A review of intraurban variations in particulate air pollution: implications for epidemiological research. Atmos Environ 39:6444–6462. https://doi.org/10.1016/j.atmosenv.2005.07.030

Wongphatarakul V, Friedlander SK, Pinto JP (1998) A comparative study of $PM_{2.5}$ ambient aerosol chemical databases. Environ Sci Technol 32(24):3926–3934. https://doi.org/10.1021/es9800582

World Health Organization (2000) Air quality guidelines for Europe, 2nd edn. https://www.who.int/publications/i/item/9789289013581

Yilmaz G (2016) Chemical characterization of micronutrients in the atmospheric particles over the Eastern Mediterranean: bio-availability and impact of atmospheric inputs on marine productivity. Dissertation, Middle East Technical University

Yin P, Brauer M, Cohen AJ, Wang H et al (2020) The effect of air pollution on deaths, disease burden, and life expectancy across China and its provinces, 1990–2017: an analysis for the Global Burden of Disease Study 2017. Lancet Planet Health 4:386–398. https://doi.org/10.1016/S2542-5196(20)30161-3

Zhang F, Chen Y, Tian C, Wang X, Huang G, Fang Y, Zong Z (2014) Identification and quantification of shipping emissions in Bohai Rim, China. Sci Total Environ 497–498:570–577. https://doi.org/10.1016/j.scitotenv.2014.08.016